Available at www.sciencedirect.com

ScienceDirect

journal homepage: www.elsevier.com/locate/he

Solid–gas and electrochemical hydrogenation properties of pseudo-binary (Ti,Zr)Ni intermetallic compounds

B. Guiose, F. Cuevas, B. Décamps, A. Percheron-Guégan*

Equipe de Chimie Métallurgique des Terres Rares, ICMPE, UMR7182, CNRS, 2-8 rue Henri Dunant, 94320 Thiais Cedex, France

ARTICLE INFO

Article history:
Received 9 June 2008
Received in revised form
16 July 2008
Accepted 17 July 2008
Available online 21 September 2008

Keywords:
Ni–MH batteries
Metal hydrides
Intermetallic compounds
TiNi
Shape memory alloys

ABSTRACT

Hydrogenation properties of pseudo-binary $Ti_{1.02-x}Zr_xNi_{0.98}$ ($0 \le x \le 0.48$) intermetallic compounds have been investigated. The substitution of Zr for Ti in TiNi compound leads to a high increase of the storage capacity both in solid–gas reaction (1.4 hydrogen atoms per formula unit, H f.u.$^{-1}$ for TiNi and 2.6 H f.u.$^{-1}$ for the substituted compounds) and electrochemical reaction (150 mAhg^{-1} for TiNi and ~350 mAhg^{-1} for the substituted compounds). The high capacity of the substituted compounds is closely linked to the martensitic transformation that occurs in TiNi-type intermetallic compounds.

1. Introduction

The TiNi compound is used in many industrial applications because of its outstanding properties of shape memory alloy [1,2]. TiNi exhibits polymorphism. The high-temperature cubic structure $Pm\bar{3}m$ (B2) transforms on cooling into a monoclinic structure $P2_1/m$ (B19′) at about 325 K for the equiatomic stoichiometry. Since the transformation is martensitic type, the high and low temperature phases are commonly denoted as austenitic and martensitic phases.

Moreover TiNi shows good hydrogen storage capacity [3], high electrochemical activity [4,5] and corrosion resistance in KOH soaking [6,7]. Burch et al. [3] have determined the hydrogenation properties of TiNi austenitic phase. TiNi absorbs up to 1.4 hydrogen atoms per formula unit (H f.u.$^{-1}$) at normal temperature and pressure. Used as negative electrode of nickel–metal hydride (Ni–MH) batteries, Gutjahr et al. have measured a reversible hydrogen capacity of about 230 mAhg^{-1} at very slow discharging rates [7].

Several authors have reported that the substitution of Zr for Ti leads to a high increase of the storage capacity [8–11]. Recently, Cuevas et al. [11] have studied $Ti_{0.64}Zr_{0.36}Ni$ compound having either pure martensitic or austenitic phases. They have showed that the martensitic phase is more interesting for hydrogen storage than the austenitic one: the former is able to store a much higher amount of hydrogen (2.6 H f.u.$^{-1}$) than the latter (1.6 H f.u.$^{-1}$).

In this paper, we focused on solid–gas and electrochemical hydrogenation properties of $Ti_{1.02-x}Zr_xNi_{0.98}$ intermetallic compounds in a wide range of Zr-content ($0 \le x \le 0.48$).

2. Experimental

We have chosen to study Ti-rich compounds to avoid variations in the martensitic transformation (MT) temperature in the case of small fluctuations in the nickel content [12]. $Ti_{1.02-x}Zr_xNi_{0.98}$ intermetallic compounds with $x = 0$, 0.12, 0.24, 0.36 and 0.48

* *Corresponding author*. Tel.: +33 149781225; fax: +33 149781203.
E-mail address: cuevas@icmpe.cnrs.fr (F. Cuevas).
0360-3199/$ – see front matter © 2008 International Association for Hydrogen Energy. Published by Elsevier Ltd. All rights reserved.
doi:10.1016/j.ijhydene.2008.07.056

Table 1 – Chemical composition and concentration of the different phases in $Ti_{1.02-x}Zr_xNi_{0.98}$ intermetallic compounds

x	Measured composition			Phase	% Phase
	Ti (% at.)	Zr (% at.)	Ni (% at.)		
0	50.0 (0.1)[a]	–	50.0 (0.1)	TiNi	94
	65.1 (1.4)	–	34.9 (1.4)	Ti_2Ni	6
0.12	44.9 (0.6)	6.0 (0.5)	49.0 (0.2)	(Ti.Zr)Ni	94
	61.1 (0.5)	5.8 (0.2)	33.1 (0.4)	$(Ti,Zr)_2Ni$	6
0.24	38.9 (0.5)	12.0 (0.5)	49.1 (0.1)	(Ti,Zr)Ni	93
	47.8 (8.3)	12.5 (3.5)	39.7 (7.2)	$(Ti,Zr)_2Ni$	5
	43.7 (4.9)	18.2 (3.4)	38.1 (3.5)	TiZrNi	2
0.36	32.8 (0.2)	17.9 (0.1)	49.3 (0.2)	(Ti,Zr)Ni	95
	48.7 (2.6)	16.6 (0.2)	34.7 (2.3)	$(Ti,Zr)_2Ni$	5
0.48	26.8 (0.3)	23.8 (0.1)	49.4 (0.3)	(Ti,Zr)Ni	94
	42.1 (1.9)	23.8 (0.1)	34.1 (1.9)	$(Ti,Zr)_2Ni$	3
	36.0 (0.5)	25.4 (0.1)	38.6 (0.5)	TiZrNi	4

a Standard deviation are given in parentheses.

have been prepared as ingots by induction melting from pure elements (purity of 99.9%). The compounds were remelted 5 times under secondary vacuum and turned over between each melting in order to ensure their homogeneity. These samples were then annealed at 1173 K during 1 week for the binary compound and 3 weeks for the substituted compounds.

The composition of the intermetallic compounds was analysed by electron probe microanalysis (EPMA) in a Cameca SX-100 operated at 15 kV. Differential scanning calorimetry (DSC) was used to determine MT temperatures in a DSC Q100TA calorimeter ranging from 313 K to 823 K, with a heating and cooling rate of 10 °C/min. The direct and reverse MT temperatures were determined at the third thermal cycle. X-ray diffraction (XRD) analyses of the compounds were performed at room temperature using a Brucker AXS D8 Advance θ–θ diffractometer, with Cu Kα radiation. For structural (XRD) and chemical (EPMA) analysis of the intermetallic compounds, the ingots were cut into plates with a low-speed diamond saw, then embedded in epoxy resin and finally mechanically polished. XRD measurements on hydrides are done with sample powders since the intermetallic compound embrittles after hydrogenation.

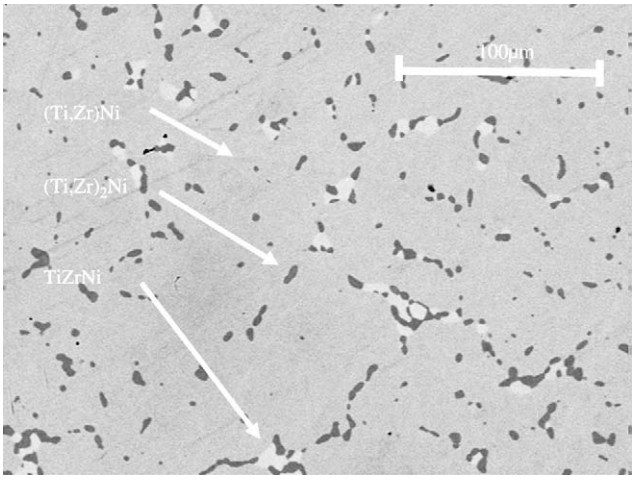

Fig. 1 – Backscattered electron micrograph of $Ti_{0.78}Zr_{0.24}Ni_{0.98}$ intermetallic compound.

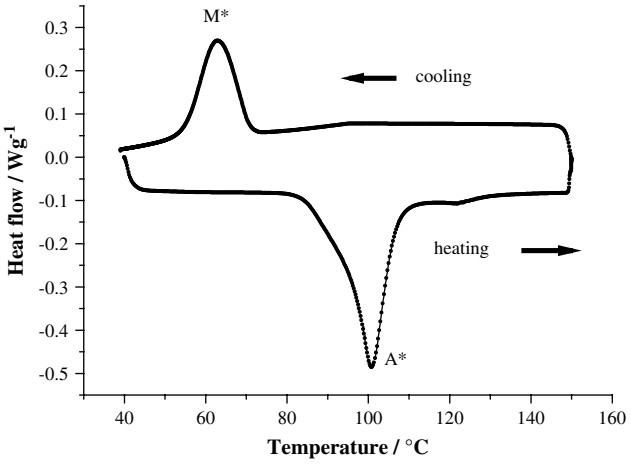

Fig. 2 – DSC curve of $Ti_{1.02}Ni_{0.98}$ binary compound. M* and A* stand for the peak temperature of direct and reverse MT, respectively.

Pressure-composition isotherms (PCI) were measured at 373 K by solid–gas reaction using the Sievert's method. Hydrogen pressures ranging from 10^{-3} MPa to 6 MPa were used. The samples were beforehand etched with 10% HF solution for 30 s to eliminate surface oxides.

Electrochemical isotherms and cycling experiments were performed using a one-compartment open cell. This electrochemical cell is composed of a negative working-electrode formed with hydride powder as active material, an $Ni(OH)_2$/NiOOH counter electrode, a polyamide insulator put between the working and the counter electrodes, and a Hg/HgO reference electrode. Hydride powder was previously sieved under 63 μm and mixed with conductive carbon and polytetrafluoroethylene (PTFE) in the weight ratio 90:5:5. The preparation was then rolled out until a thickness of 0.25 mm and then compressed on Ni grids. Electrochemical cycling experiments were performed in galvanostatic mode using a MacPile II device from Bio Logic at a regime of C/10. The cut-off potential was fixed at −0.7 V vs. Hg/HgO. The electrodes were allowed to relax for 0.5 h before current inversion. Discharging electrochemical isotherms at room temperature were obtained by the galvanostatic intermittent titration technique (GITT) using relaxation times of 1 h to reach the open-circuit equilibrium potential.

Table 2 – Direct (M*) and reverse (A*) MT temperatures and difference between M* and A* for $Ti_{1.02-x}Zr_xNi_{0.98}$ intermetallic compounds (with $0 \le x \le 0.48$)

x	M* (°C)	A* (°C)	A* − M* (°C)
0	57	93	36
0.12	46	112	66
0.24	105	165	60
0.36	231	278	47
0.48	345	415	70

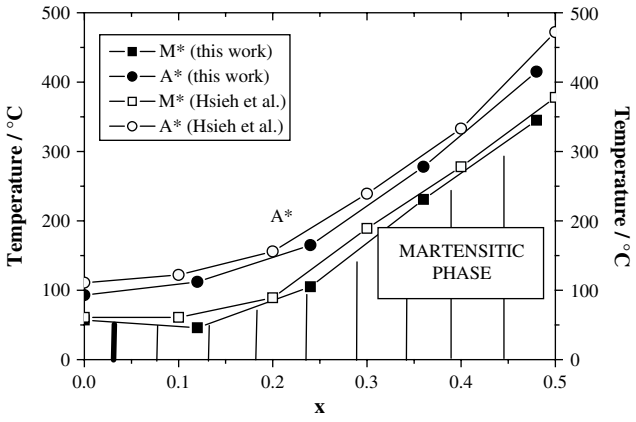

Fig. 3 – Dependence of MT temperatures as a function of Zr-content in this work and by Hsieh et al. [11]. M^* and A^* correspond to direct and reverse MT temperatures, respectively. The hatched area represents the region of existence of the martensitic phase.

3. Results and discussion

3.1. *Chemical and structural characterisation of intermetallic compounds*

The chemical composition of the intermetallic compounds obtained by EPMA is given in Table 1. The samples are composed of a major (Ti,Zr)Ni phase and a small amount of one secondary $(Ti,Zr)_2Ni$ phase for $x = 0$, 0.12 and 0.36, and two secondary $(Ti,Zr)_2Ni$ and TiNiZr phases for $x = 0.24$ and 0.48. In all cases, the amount of secondary phases (i.e. $(Ti,Zr)_2Ni$ and TiNiZr) is estimated to be about 6%, as determined by Image J analysis software. According to the Ti–Ni phase diagram [10], the precipitation of $(Ti,Zr)_2Ni$ phase is expected in Ti-rich TiNi-type compounds. Moreover, the major phase is observed to be equi-stoichiometric for the binary compound. As for the substituted compounds, the nickel content deviates systematically (49.2 ± 0.2 at%) with respect to the equi-stoichiometric value. TiNiZr phases have already been reported to precipitate in (Ti,Zr)Ni compounds [13,14]. An example ($x = 0.24$) of the compounds' microstructure with the three observed phases is shown in Fig. 1. In EPMA backscattering electron images, bright areas indicate phases with high electronic density (i.e. containing elements with high atomic number), whereas dark areas correspond to phases with low electronic densities. It should be noted that the sizes of $(Ti,Zr)_2Ni$ and TiNiZr precipitates are close to the spatial resolution of the EPMA analysis (typically $\sim 1\,\mu m$) so that the given chemical composition (Table 1) for the secondary phases may have a large error.

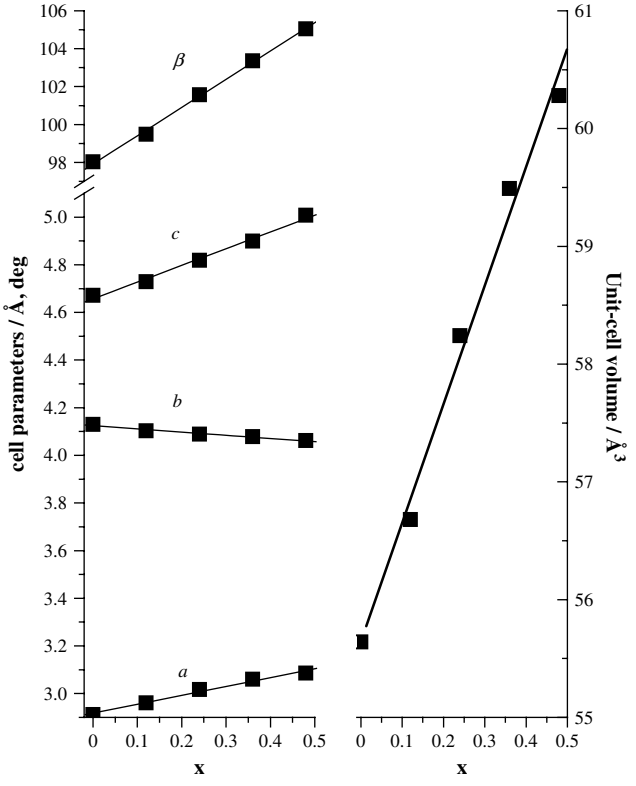

Fig. 4 – Dependence of lattice parameters *a*, *b*, *c*, β and unit-cell volume *V* of the major (Ti,Zr)Ni phase as a function of Zr-content in $Ti_{1.02-x}Zr_xNi_{0.98}$ intermetallic compounds. Straight lines are the best linear fit to the data.

Fig. 2 shows DSC measurements for the $Ti_{1.02}Ni_{0.98}$ binary compound. Only one peak is observed during both heating and cooling, which correspond to the reverse and direct MT temperatures, respectively. One-stage martensitic transformation is a common feature of Ti-rich TiNi compounds [15,16].

The MT temperatures taken at the top of each peak (labelled as A^* and M^* for reverse and direct MT, respectively) and the temperature difference between them are given in Table 2. The MT temperatures in dependence of Zr-content are plotted in Fig. 3. For $x = 0.12$, MT temperatures are close to those of the binary compound. On the contrary, from $x = 0.24$ to $x = 0.48$, MT temperatures (M^* and A^*) rise linearly as a function of Zr-content. Therefore, the martensitic phase range widens in temperature with increasing Zr-content as seen in Fig. 3. For comparison, DSC data from Hsieh et al. [13] on $Ti_{1.03-x}Zr_xNi_{0.97}$ intermetallic compounds are also displayed in Fig. 3. The MT temperatures observed by these authors are in close agreement with our data, but our values are slightly lower.

The above reported DSC measurements indicate that the intermetallic compounds are in the martensitic phase at room temperature. This is confirmed by XRD measurements at room temperature (not shown) since the diffraction peaks corresponding to the major (Ti,Zr)Ni phase can be indexed in the monoclinic $P2_1/m$ space group. Fig. 4 shows the dependence of lattice parameters *a*, *b*, *c*, β and cell volume *V* with Zr-content of the major (Ti, Zr)Ni phase. An anisotropic behaviour in the lattice parameters is observed. In fact, *a*, *c* and β increase linearly whereas *b* decreases with increasing Zr-content. A similar behaviour has been reported in the literature [14,17]. A linear increase of the cell volume as a function of the Zr atomic concentration is also observed. This is attributed to the larger atomic radius of Zr (1.60 Å) with respect to Ti (1.47 Å). This linear increase is in agreement with the Vegard's rule governing solid solutions.

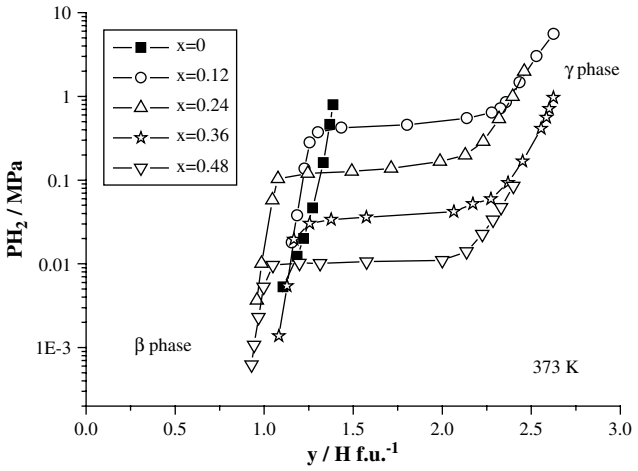

Fig. 5 – Desorption PCI curves at 373 K of $Ti_{1.02-x}Zr_xNi_{0.98}$ compounds (with $0 \le x \le 0.48$).

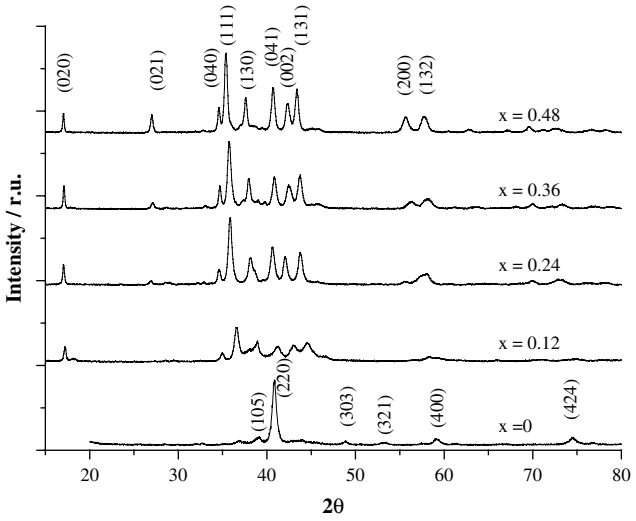

Fig. 7 – Comparison of XRD patterns of $Ti_{1.02}Ni_{0.98}H_{1.4}$ and $Ti_{1.02-x}Zr_xNi_{0.98}H_{2.6}$ ($0.12 \le x \le 0.48$) hydrides indexed in *I4/mmm* and *Cmcm* space group, respectively.

3.2. *Solid–gas hydrogenation properties*

Desorption PCI curves at 373 K in the pressure range 10^{-3}–10 MPa for all the studied compounds are displayed in Fig. 5. A different behaviour is observed between the binary and the substituted compounds. For the binary compound, hydrogen content $TiNiH_y$ increases continuously with pressure from $y = 1$ H f.u.$^{-1}$ to $y = 1.4$ H f.u.$^{-1}$, following therefore, a solid-solution behaviour in agreement with Burch et al. [3]. This solid solution occurs in the β-hydride phase previously reported by Soubeyroux et al. [18]. On the contrary, the substituted compounds exhibit a wide plateau pressure. This plateau reveals the coexistence of two hydrides for $1 < y < 2.2$, which will be named as β and γ phases, with γ the hydride having the highest content of hydrogen. The maximum content for the γ-hydride phase is $y = 2.6$ H f.u.$^{-1}$. It is worth to note that the β-hydride phase is very stable. It does not decompose for hydrogen pressures as low as 10^{-3} MPa.

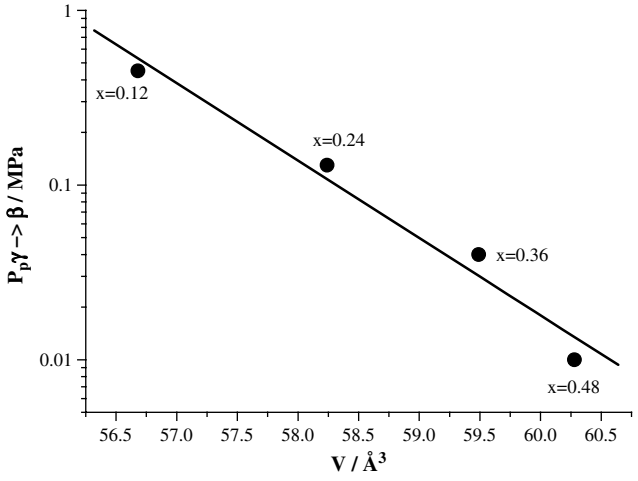

Fig. 6 – Variation of the desorption plateau pressure (γ → β) with the unit-cell volume of $Ti_{1.02-x}Zr_xNi_{0.98}$ ($0.12 \le x \le 0.48$) intermetallic compounds at 373 K.

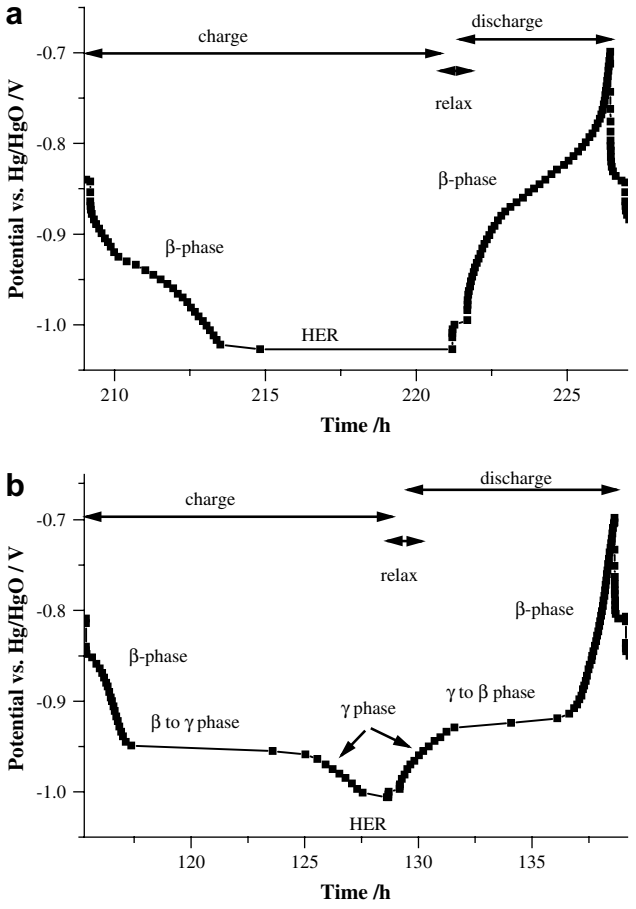

Fig. 8 – Typical variation of the electrochemical potential for (a) binary compound and (b) $Ti_{1.02-x}Zr_xNi_{0.98}$ ($0.12 \le x \le 0.48$) substituted compounds.

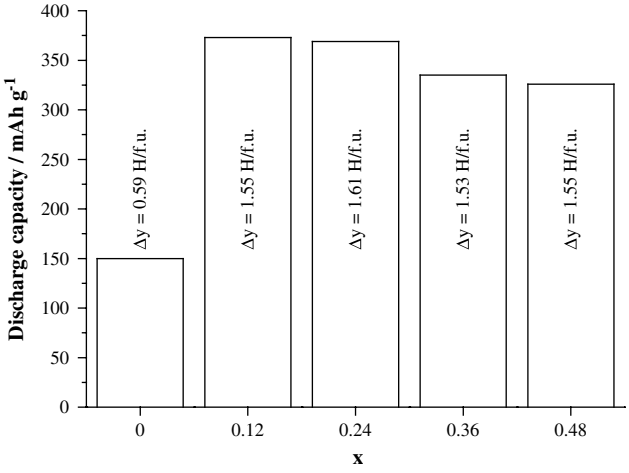

Fig. 9 – Maximal electrochemical discharge capacity of $Ti_{1.02-x}Zr_xNi_{0.98}$ ($0 \le x \le 0.48$) compounds. The equivalent number of electrochemically desorbed hydrogen atoms per formula unit, Δy, is also given.

The dependence of the γ → β desorption plateau pressure with the unit-cell volume of the intermetallic compounds is shown in Fig. 6. The logarithm of the plateau pressure linearly decreases with the intermetallic unit-cell volume in agreement with the empirical geometric model [19].

PCI curves have also been measured at room temperature for $x = 0.12$ compound to determine whether substituted compounds can be electrochemically loaded in open-cell systems. The absorption and desorption β ↔ γ plateau pressure at room temperature are 4×10^{-2} MPa and 1.4×10^{-2} MPa, respectively. Since the absorption plateau pressure is lower than 0.1 MPa and this compound forms the less stable hydrides, it can be concluded that all substituted compounds can be hydrogenated up to the γ-phase in open-cell systems.

XRD patterns of hydrides at the maximum hydrogen loading are shown in Fig. 7. The crystal structure of the $Ti_{1.02}Ni_{0.98}H_{1.4}$ hydride and the $Ti_{1.02-x}Zr_xNi_{0.98}H_{2.6}$

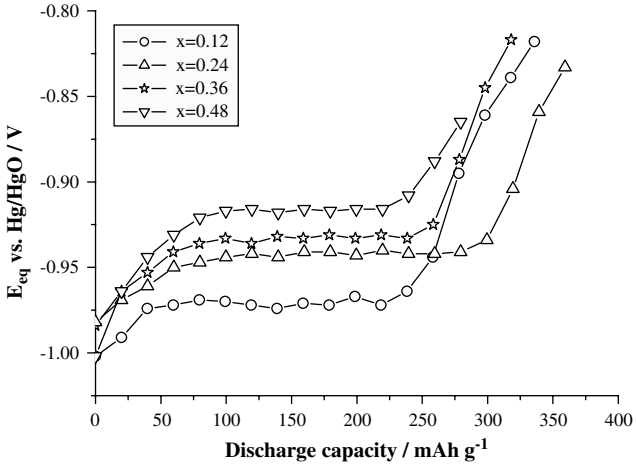

Fig. 10 – Electrochemical discharging isotherms of $Ti_{1.02-x}Zr_xNi_{0.98}$ ($0.12 \le x \le 0.48$) substituted compounds at room temperature.

Table 3 – Electrochemical equilibrium plateau potential, E_{eq}, equivalent electrochemical pressure, $P_{p,el}$, and solid–gas plateau pressure, $P_{p,sg}$, for the γ → β transition in $Ti_{1.02-x}Zr_xNi_{0.98}$ ($0.12 \le x \le 0.48$) compounds

Composition	E_{eq} (mV)	$P_{p,el}$ (MPa)	$P_{p,sg}$ (MPa)
$Ti_{0.90}Zr_{0.12}Ni_{0.98}$	−970	10^{-2}	1.4×10^{-2}
$Ti_{0.78}Zr_{0.24}Ni_{0.98}$	−940	4×10^{-3}	–
$Ti_{0.66}Zr_{0.36}Ni_{0.98}$	−930	2×10^{-3}	7.6×10^{-4}[a]
$Ti_{0.54}Zr_{0.48}Ni_{0.98}$	−916	1.6×10^{-4}	–

a This value refers to Cuevas et al. study on $Ti_{0.64}Zr_{0.36}Ni$ compound [9]. It is calculated by extrapolation of the given Van't Hoff plot to room temperature.

($0.12 \le x \le 0.48$) compounds differ considerably. The structure of $Ti_{1.02}Ni_{0.98}H_{1.4}$ hydride can be described as a super-cell ($2a \times 4a$) structure of the cubic austenitic phase. This hydride has a tetragonal structure (space group *I4/mmm*) with cell parameter $a = b = 6.235(2)$ Å and $c = 12.447(7)$ Å. These results are in agreement with those reported in the literature [18,20]. The XRD patterns of all the substituted hydrides correspond to an orthorhombic structure with space group *Cmcm*. The diffraction lines shift toward lower angles with increasing Zr-content due to the increase of the unit-cell volume induced by the Zr-substitution. The change of the monoclinic structure for the intermetallic compound into a base-centered orthorhombic one for the hydrides may be explained by a small change of the β angle from 98 to 108° [21].

3.3. *Electrochemical hydrogenation properties*

Fig. 8 displays the typical variation of the electrochemical potential for binary (Fig. 8a) and substituted compounds (Fig. 8b) for selected galvanostatic cycles. For the binary compound, the potential continuously decreases during the charging cycle till reaching a plateau potential. Such a continuous decrease is attributed, by comparison with the PCI desorption curve for this compound (Fig. 5), to hydrogen absorption in the β-hydride phase. The plateau potential, located at about −1.02 V, corresponds to the hydrogen evolution reaction (HER). On discharging, hydrogen desorption from the β-hydride phase takes place. As for the substituted compounds, a first plateau potential occurs on charging between two decreasing potential branches. This plateau is attributed to the β → γ phase transformation (see PCI curves in Fig. 5). The HER reaction is observed at the end of the charging cycle. On discharge, the reverse phase transition (γ → β) is identified.

The electrochemical discharge capacity of the $Ti_{1.02-x}Zr_xNi_{0.98}$ ($0 \le x \le 0.48$) compounds cycled in 8 M KOH is shown in Fig. 9. The capacities of the binary compound $Ti_{1.02}Ni_{0.98}$ and $Ti_{1.02-x}Zr_xNi_{0.98}$ ($0.12 \le x \le 0.48$) substituted compounds differ considerably. The maximum capacity of the binary compound reaches only 150 $mAhg^{-1}$ whereas for the substituted compounds the capacity is much higher and reaches 370 $mAhg^{-1}$ for $x = 0.12$. The number of electrochemically desorbed hydrogen atoms per formula unit, Δy, as evaluated from the measured discharge capacities, is $\Delta y = 0.6$ for the binary compound and about $\Delta y = 1.6$ for the

substituted compounds. These values are in close agreement with solid–gas PCI measurements (Fig. 5) if one considers the maximum hydrogen capacity ($y_{max} = 1.4$ H f.u.$^{-1}$ and 2.6 H f.u.$^{-1}$ for binary and intermetallic compounds, respectively) and the high stability of the β-hydrides in both kinds of compounds. As a matter of fact, the hydrogen stored at $y \leq 1$ H f.u.$^{-1}$ is strongly bonded in β-hydrides for all the studied compounds and does not participate in reversible electrochemical loading.

Discharging electrochemical isotherms were measured at room temperature for the $Ti_{1.02-x}Zr_xNi_{0.98}$ ($0.12 \leq x \leq 0.48$) substituted compounds (Fig. 10). The isotherms exhibit a plateau potential which become less negative with the increasing of Zr-content. Thus, the plateau potential increases from −970 mV for $x = 0.12$ to −916 mV for $x = 0.48$. Using the Nernst equation, the equivalent electrochemical plateau pressure, $P_{p,el}$, can be calculated and compared with the plateau pressure of the γ → β phase transition determined by solid–gas measurements, $P_{p,sg}$. Such a comparison is given in Table 3. The electrochemical plateau potentials are in agreement with the solid–gas measurements as expected from the thermodynamic equivalence between the solid–gas and electrochemical reactions. Consequently, the first potential raise (Fig. 10) corresponds to hydrogen discharge from the γ hydride. Then, the plateau potential corresponds to the two phase coexistence region (γ and β-hydrides). Finally, the last potential rise involves the discharge of hydrogen from the β hydride.

4. Conclusion

Polymorphism in (Ti,Zr)Ni-type intermetallic compounds has a huge influence on both electrochemical and solid–gas hydrogenation properties. For the substituted compounds, which form hydrides related to the martensitic phase, PCI curves reveal the existence of a wide plateau pressure, reflecting the coexistence of two hydrides (β and γ). The results of our research have shown that (Ti,Zr)Ni martensitic compounds can store a high amount of hydrogen (2.6 H f.u.$^{-1}$). In contrast, the binary compound, which forms a hydride related to the austenitic phase, exhibits no plateau pressure in its PCI curve and the maximum capacity is poor (1.4 H f.u.$^{-1}$). The equivalence between electrochemical and solid–gas loading has been demonstrated. Substituted compounds have an electrochemical capacity of about 350 mAhg^{-1} (i.e. ∼1.6 H f.u.$^{-1}$) against only ∼150 mAhg^{-1} (i.e. ∼0.6 H f.u.$^{-1}$) for the binary compound. The difference of the obtained capacity between electrochemical and solid–gas measurement is about 1 H f.u.$^{-1}$ which corresponds to the existence of non-reversible hydrogen atoms in the β-hydride phase that do not participate in the electrochemical process. Therefore, substituted compounds are more relevant than the binary compound for storage applications.

Acknowledgements

The authors wish to thank E. Leroy for EPMA analysis.

REFERENCES

[1] Otsuka K, Ren X. Recent developments in the research of shape memory alloys. Intermetallics 1999;7:511–28.
[2] Otsuka K, Ren X. Physical metallurgy of Ti–Ni based shape memory alloys. Prog Mater Sci 2005;50:511–678.
[3] Burch R, Mason NB. Absorption of hydrogen by titanium–cobalt and titanium–nickel intermetallic alloys. J Chem Soc Faraday Trans I 1979;75:561–77.
[4] Panek J, Serek A, Budniok A, Rówinski E, Lagiewka E. Ni + Ti composite layers as cathode materials for electrolytic hydrogen evolution. Int J Hydrogen Energy 2003;28:169–75.
[5] Kellenberg A, Vaszilcsin N, Brandl W, Duteanu N. Kinetics of hydrogen evolution reaction on skeleton nickel and nickel–titanium electrodes obtained by thermal arc spraying technique. Int J Hydrogen Energy 2007;32:3258–65.
[6] Justi EW, Ewe HH, Kalberlah AW, Saridakis NM, Schaefer MH. Electrocatalysis in the nickel–titanium system. Energy Convers 1970;10:183–7.
[7] Gutjahr MA, Buchner H, Beccu KD, Säufferer H. A new type of reversible negative electrode for alkaline storage batteries based on metal alloy hydrides. Power Sources 1973;4:79–91.
[8] Wakao S, Sawa H, Nakano H, Chubachi S, Abe M. Capacities and durabilities of Ti–Zr–Ni alloy hydride electrodes and effects of electroless plating on their performances. J Less-Common Met 1987;131:311–9.
[9] Bouet J, Knosp B, Percheron-Guégan A, Jordy C. Matériau hydrurable pour électrode négative d'accumulateur nickel–hydrure et son procédé de préparation. French patent 9206732; 1992.
[10] Jordy C, Latroche M, Percheron-Guégan A, Achard J-C, Bouet J, Knosp B, et al. Effect of partial substitution in TiNi on its structural and electrochemical hydrogen storage properties. Z Phys Chem 1994;185:119–30.
[11] Cuevas F, Latroche M, Ochin P, Dezellus A, Fernandez J-F, Sanchez C, et al. Influence of the martensitic transformation on the hydrogenation properties of $Ti_{50-x}Zr_xNi_{50}$ alloys. J Alloys Compd 2002;330-332:250–5.
[12] Murray J-L. The Ni–Ti (nickel–titanium) system. In: Murray J-L, editor. Phase diagrams of binary titanium alloys. Metals Park, Ohio: ASM Internationall; 1987. p. 197–211.
[13] Hsieh SF, Wu SK. A study on ternary Ti-rich TiNiZr shape memory alloys. Mater Charact 1998;41:151–62.
[14] Mulder JH. Investigation of high temperature shape memory alloys from Ni–Ti–Zr and Ni–Ti–Hf systems. PhD thesis, University of Twente, Enschede; 1995. p. 150.
[15] Wade N, Adachi Y, Hosoi Y. A role of hydrogen in shape memory effect in Ti–Ni alloys. Scr Metall Mater 1990;24:1051–5.
[16] Lin HC, Wu SK, Lin JC. The martensitic transformation in Ti-rich TiNi shape memory alloys. Mater Chem Phys 1994;37:184–90.
[17] Hsieh SF, Wu SK. A study on lattice parameters of martensite in $Ti_{50.5-x}Ni_{49.5}Zr_x$ shape memory alloys. J Alloys Compd 1998;270:237–41.
[18] Soubeyroux J-L, Fruchart D, Lorthioir G, Ochin P, Colin D. Structural study of the hydrides $NiTiH_x$ ($x = 1.0$ and 1.4). J Alloys Compd 1993;196:127.
[19] Achard J-C, Percheron-Guégan A, Diaz H, Briaucourt F, Demany F. Rare earth ternary hydrides. Hydrogen storage applications. In: Presented at second international congress on hydrogen in metals, Paris, 1E12; 1977.
[20] Noréus D, Werner P-E, Alasafi K, Schmidt-Ihn E. Structural studies of TiNiH. Int J Hydrogen Energy 1985;10:547.
[21] Cuevas F, Latroche M, Bourée-Vigneron F, Percheron-Guégan A. A conjoint XRD-ND analysis of the crystal structures of austenitic and martensitic $Ti_{0.64}Zr_{0.36}Ni$ hydrides. J Solid State Chem 2006;179:3295–307.